

2011

Communication: New insight into the barrier governing CO₂ formation from OH + CO

Christopher J. Johnson
University Of California

Berwyck L. Poad
University of Wollongong, bpoad@uow.edu.au

Ben B. Shen
University Of California

Robert E. Continetti
University Of California

Follow this and additional works at: <https://ro.uow.edu.au/scipapers>



Part of the [Life Sciences Commons](#), [Physical Sciences and Mathematics Commons](#), and the [Social and Behavioral Sciences Commons](#)

Recommended Citation

Johnson, Christopher J.; Poad, Berwyck L.; Shen, Ben B.; and Continetti, Robert E.: Communication: New insight into the barrier governing CO₂ formation from OH + CO 2011.
<https://ro.uow.edu.au/scipapers/4617>

Communication: New insight into the barrier governing CO₂ formation from OH + CO

Abstract

Despite its relative simplicity, the role of tunneling in the reaction $\text{OH} + \text{CO} \rightarrow \text{H} + \text{CO}(2)$ has eluded the quantitative predictive powers of theoretical reaction dynamics. In this study a one-dimensional effective barrier to the formation of $\text{H} + \text{CO}(2)$ from the HOCO intermediate is directly extracted from dissociative photodetachment experiments on HOCO and DOCO. Comparison of this barrier to a computed minimum-energy barrier shows that tunneling deviates significantly from the calculated minimum-energy pathway, predicting product internal energy distributions that match those found in the experiment and tunneling lifetimes short enough to contribute significantly to the overall reaction. This barrier can be of direct use in kinetic and statistical models and aid in the further refinement of the potential energy surface and reaction dynamics calculations for this system.

Keywords

barrier, into, formation, governing, oh, insight, co, communication, co₂, GeoQUEST

Disciplines

Life Sciences | Physical Sciences and Mathematics | Social and Behavioral Sciences

Publication Details

Johnson, C. J., Poad, B. L., Shen, B. B. & Continetti, R. E. (2011). Communication: New insight into the barrier governing CO₂ formation from OH + CO. *Journal of Chemical Physics*, 134 (17), 171106-1-171106-4.

Communication: New insight into the barrier governing CO₂ formation from OH + CO

Christopher J. Johnson, Berwyck L. J. Poad, Ben B. Shen, and Robert E. Continetti

Citation: *J. Chem. Phys.* **134**, 171106 (2011); doi: 10.1063/1.3589860

View online: <http://dx.doi.org/10.1063/1.3589860>

View Table of Contents: <http://jcp.aip.org/resource/1/JCPSA6/v134/i17>

Published by the [American Institute of Physics](#).

Additional information on *J. Chem. Phys.*

Journal Homepage: <http://jcp.aip.org/>

Journal Information: http://jcp.aip.org/about/about_the_journal

Top downloads: http://jcp.aip.org/features/most_downloaded

Information for Authors: <http://jcp.aip.org/authors>

ADVERTISEMENT



**ACCELERATE COMPUTATIONAL CHEMISTRY BY 5X.
TRY IT ON A FREE, REMOTELY-HOSTED CLUSTER.**

[LEARN MORE](#)

Communication: New insight into the barrier governing CO₂ formation from OH + CO

Christopher J. Johnson,¹ Berwyck L. J. Poad,² Ben B. Shen,² and Robert E. Continetti^{2,a)}

¹*Department of Physics, University of California San Diego, 9500 Gilman Dr., La Jolla, California 92093-0354, USA*

²*Department of Chemistry and Biochemistry, University of California San Diego, 9500 Gilman Dr., La Jolla, California 92093-0340, USA*

(Received 24 March 2011; accepted 20 April 2011; published online 6 May 2011)

Despite its relative simplicity, the role of tunneling in the reaction $\text{OH} + \text{CO} \rightarrow \text{H} + \text{CO}_2$ has eluded the quantitative predictive powers of theoretical reaction dynamics. In this study a one-dimensional effective barrier to the formation of $\text{H} + \text{CO}_2$ from the HOCO intermediate is directly extracted from dissociative photodetachment experiments on HOCO and DOCO. Comparison of this barrier to a computed minimum-energy barrier shows that tunneling deviates significantly from the calculated minimum-energy pathway, predicting product internal energy distributions that match those found in the experiment and tunneling lifetimes short enough to contribute significantly to the overall reaction. This barrier can be of direct use in kinetic and statistical models and aid in the further refinement of the potential energy surface and reaction dynamics calculations for this system. © 2011 American Institute of Physics. [doi:10.1063/1.3589860]

The elementary reaction $\text{OH} + \text{CO} \rightarrow \text{H} + \text{CO}_2$ has been the subject of extensive theoretical and experimental studies, yet the detailed dynamics remain poorly understood. This reaction governs CO/CO₂ ratios in hydrocarbon combustion and the upper atmosphere, and impacts the HO_x/NO_x/SO_x atmospheric cycles through the destruction of OH radicals.¹ It is one of the simplest complex-forming elementary reactions; it is strongly exothermic but features a very stable intermediate, HOCO, and a barrier to activation in the product channel of roughly similar energy to the reactants.^{2–4} As a four-atom system, the $\text{OH} + \text{CO} \rightarrow \text{HOCO} \rightarrow \text{H} + \text{CO}_2$ reaction is amenable to a broad range of theoretical treatments,^{2,5–8} and several high-level potential energy surfaces (PESs) exist.^{9–13} The reaction proceeds through the strongly bound *cis*-HOCO intermediate¹⁴ and shows striking non-Arrhenius behavior.³ The exact height and shape of the barrier to the formation of $\text{H} + \text{CO}_2$ are critical to the overall kinetics of the reaction. However, beyond limited spectroscopic studies^{15–21} and measurements of excited state dynamics,²² little experimental information exists on the isolated HOCO radical, and there is no quantitative agreement on the nature of the barrier and the role that tunneling plays in the overall kinetics of the $\text{OH} + \text{CO}$ reaction.^{9,23–25}

Photoelectron-photofragment coincidence (PPC) spectroscopy²⁶ has been used to directly probe the HOCO PES governing the dynamics of this reaction, resolving three processes: detachment to internally excited HOCO radicals (stable channel), dissociation to $\text{H} + \text{CO}_2$ (exit channel), and dissociation to $\text{OH} + \text{CO}$ (entrance channel).^{27,28} All dissociation to $\text{H} + \text{CO}_2$ was found to occur below the calculated barrier on the neutral PES, consistent with tunneling dissociation. Further analysis revealed dissociation to $\text{OH} +$

CO with lifetimes less than 9×10^{-13} s, indicating that when energetically allowed, this process is facile.²⁹ However, these results were complicated by the presence of strong hot bands evident in the photoelectron spectra. Recent incorporation of a cryogenic electrostatic ion beam trap, providing internally cold anions, allowed for unprecedented insight into these dynamics, confirming the occurrence of tunneling through the exit-channel barrier.³⁰ Energy-resolved branching fractions were measured for the three processes, revealing a range of internal energy in which tunneling lifetimes to $\text{H} + \text{CO}_2$ are similar to the timescale of the experiment indicative of competition between the stable and exit channels. In the present work these studies are extended to the deuterated DOCO radical³¹ and the set of energy-resolved branching fractions are analyzed in detail in the tunneling regime, enabling the development and optimization of a realistic one-dimensional (1D) potential barrier that accurately reproduces the observed tunneling dynamics and independently predicts the observed product internal energy distributions.

The PPC spectra for $\text{HOCO}^-(\text{DOCO}^-) + h\nu \rightarrow \text{H}(\text{D}) + \text{CO}_2 + e^-$ in Fig. 1 provide the primary evidence for the presence of tunneling in the exit channel. All dissociation to $\text{H} + \text{CO}_2$ occurs above the maximum electron kinetic energy (eKE) limit denoted by horizontal lines and, barring significant errors in the computed surfaces, is therefore due entirely to tunneling. However, an interesting horizontal feature is present in both spectra at the high eKE (low energy on the PES) limit. In dissociative systems PPC spectra generally exhibit diagonal features due to the correlation of energy in the system to energy along the dissociative coordinate. The transition from diagonal to horizontal character at the high eKE limit of both spectra indicates that the tunneling lifetime approaches the time-of-flight (TOF) of the translational spectrometer, 7.8 μs for HOCO and 7.9 μs for DOCO, at these energies. If a metastable HOCO* neutral travels a significant

^{a)} Author to whom correspondence should be addressed. Electronic mail: rcontinetti@ucsd.edu.

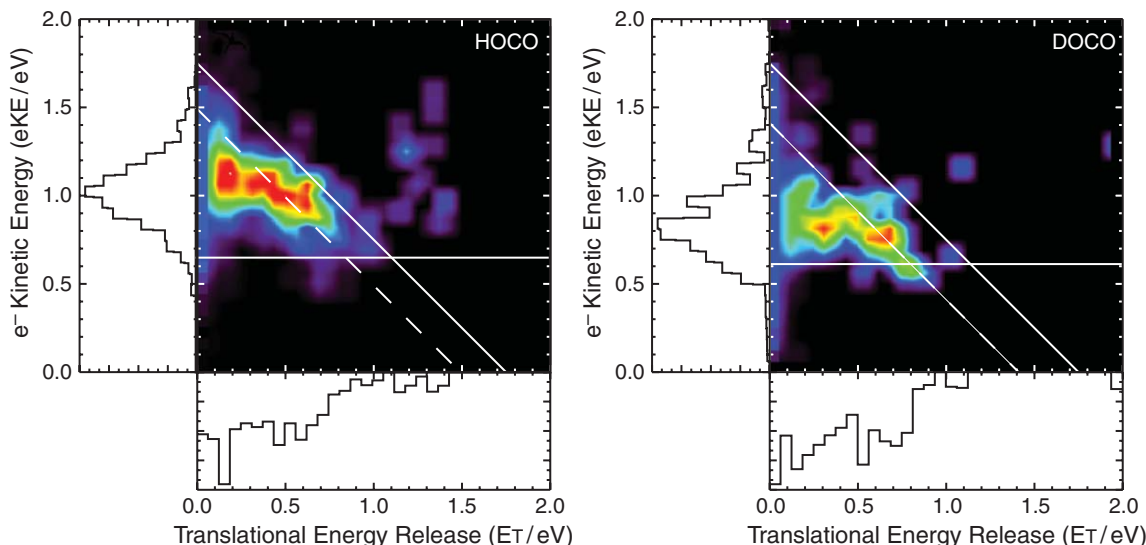


FIG. 1. PPC spectra for $\text{HOCO}^- (\text{DOCO}^-) \rightarrow \text{H}(\text{D}) + \text{CO}_2 + e^-$, corrected for the finite acceptance of the neutral particle detector. (See Ref. 37.) Solid diagonal lines indicate the calculated maximum total kinetic energy available to the system, dashed diagonal lines denote the observed product internal energy peak, and horizontal lines indicate the maximum eKE expected for above-barrier dissociation of *cis*-HOCO(DOCO). The signal above the maximum kinetic energy line is due to a small number of false coincidences and is ignored.

portion of the TOF before dissociating, the measured translational energy release (E_T) is reduced, and thus a discrete E_T is mapped into a band of apparent E_T extending from the actual value to zero. This horizontal feature appears at lower eKE (higher E_{int}) in the DOCO spectrum as expected due to the reduction in tunneling probability from the larger reduced mass of $\text{D} + \text{CO}_2$. The spectra are also shifted below the maximum total energy release (diagonal lines), indicating that 0.1–0.4 eV of the available energy is stored as internal energy in the CO_2 product.

Energy-resolved branching fractions are determined from the relative contribution of each product channel at a given energy to the overall photoelectron spectrum.³¹ In the region of competition between the stable channel and the exit channel, the stable fraction can be used to compute tunneling probabilities. A 1D barrier to dissociation can be optimized to fit these tunneling probabilities using a quasi-1D model,³¹ simplified from one outlined by Miller.³² In this model nuclear motion is assumed to be separable into dissociative and non-dissociative components and dissociative motion is treated as a two-body 1D system (H-OCO). All non-dissociative internal energy resides entirely in OCO and the partitioning of this energy is controlled by an experimentally determined parameter χ , while only dissociative energy is considered for tunneling through the barrier. The experimentally derived potential is composed of a Morse oscillator coupled to a dissociative potential, and is plotted in Fig. 2 along with a fully relaxed, zero-point corrected scan of the energy along the OH bond length using the CCSD/aug-cc-pVTZ level of theory.³³

Comparison of the experimental barrier with the computed minimum-energy barrier shows good agreement for the bound part of the surface and distinct differences for the dissociative part. The curvature parameter of the Morse potential gives an OH stretching frequency of 3486 cm^{-1} , in good agreement with the computed value.³¹ The zero-point corrected barrier height is found to be 1.13 eV at 1.44 Å,

displaced to larger r_{OH} by 0.09 Å and 0.02 eV higher than the minimum-energy barrier but significantly wider. Among the available full PESs,^{10–13} ZPE-corrected saddle points range from 0.97 to 1.28 eV, consistent with the model barrier.

The computed minimum energy barrier is not expected to properly reproduce the tunneling dynamics in the HOCO system. Calculations show significant geometrical changes as the system crosses the barrier, particularly in the OCO angle, which changes by nearly 40° over a 0.05 Å change in r_{OH} . Thus, relaxed scans along r_{OH} reflect these geometrical changes and represent a lower limit, at each bond length, to

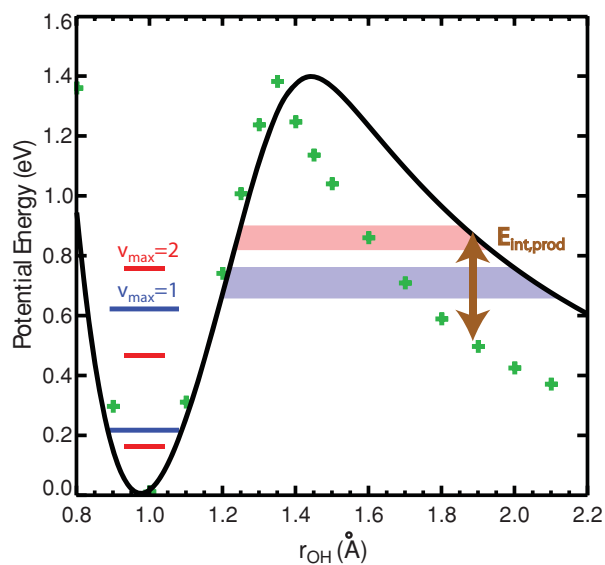


FIG. 2. Model PES for *cis*-HOCO \rightarrow H + CO_2 , shown in black, and calculated minimum-energy barrier (green crosses). Also included are the relevant OH (blue) and OD (red) vibrational levels and the range of E_{diss} where long-lifetime tunneling is observed for each isotopologue. An example of expected product internal energy, given by $E_{\text{int,prod}}$, is also shown.

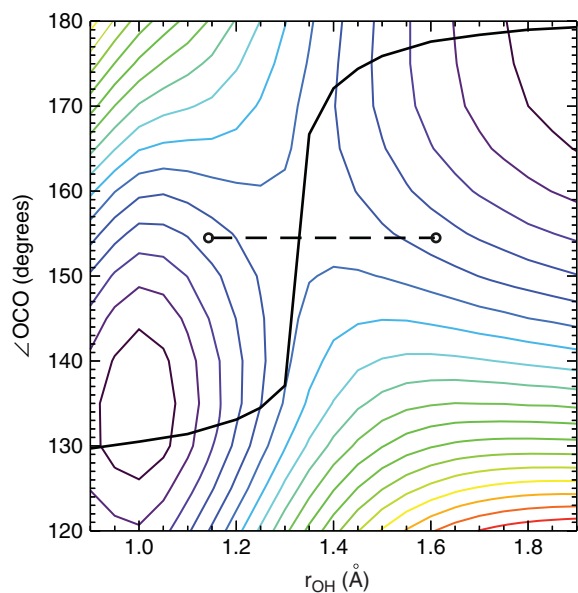


FIG. 3. An example 2D slice ($r_{\text{OH}}, \angle_{\text{OCO}}$) at fixed $r_{\text{OC}} = r_{\text{CO}} = 1.18 \text{ \AA}$ of the HOCO PES (non-ZP corrected). The computed minimum energy path (solid) is overlaid and the path of highest tunneling probability (dashed) is shown for an example value of E_{diss} .

the barrier through which tunneling occurs. Since H atom tunneling occurs rapidly compared to the motion of OCO, tunneling must occur at essentially constant CO₂ geometry, and therefore is nearly perpendicular to the minimum-energy pathway in the relevant ($r_{\text{OH}}, \angle_{\text{OCO}}$) plane of the surface, exemplified in Fig. 3.

Using the model barrier the internal energy in the CO₂ products resulting from tunneling can be estimated and compared to the experimental values. Significant vibrational excitation in the CO₂ product is expected due to the difference between the tunneling geometry and the equilibrium CO₂ geometry. Thus, the energy at the outer limit of the tunneling path gives an estimate of the internal energy in the CO₂ fragment. The difference between the calculated and experimentally derived barriers in the repulsive region is $\sim 0.2\text{--}0.3 \text{ eV}$, arising from the un-relaxed nature of the OCO fragment during tunneling. Comparison of this expectation with the average internal energy from the coincidence spectra of 0.2 eV for HOCO and 0.3 eV for DOCO shows close agreement. A second independent confirmation involves the energy partitioning factor χ relating total internal energy to internal energy in the bond-breaking coordinate. While the quasi-1D model implicitly requires vibrational adiabaticity, this is not enforced in the extraction procedure. This implies that the CO₂ fragment internal energy, once dissociation is complete, should equal the non-dissociative energy component, $E_{\text{int}} - E_{\text{diss}}$, which also ranges from 0.1 to 0.3 eV . The agreement of both of these checks without inclusion of experimental information regarding the product internal energy provides strong evidence that the model captures most of the important dynamical aspects of the system. The slight discrepancy in the internal energy distribution ranges from the model indicate that vibrational adiabaticity does not strictly hold, with partitioning of energy between kinetic and internal degrees of freedom as the OCO

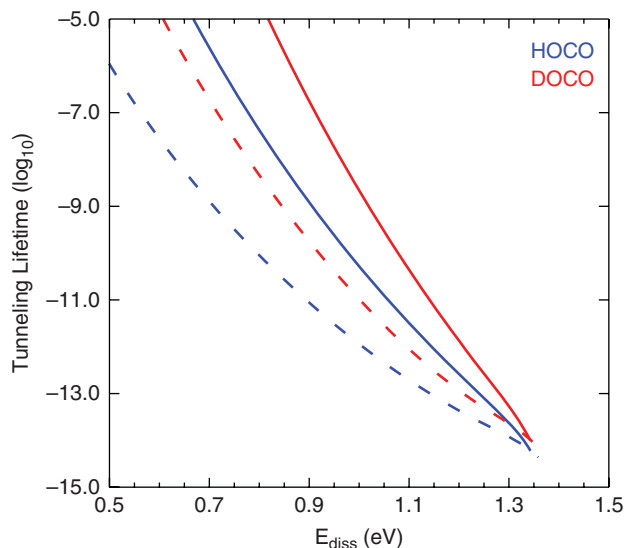


FIG. 4. Prediction of tunneling lifetimes as a function of energy in the OH (red) and OD (blue) stretch (solid lines) compared to those taken from the theoretically predicted minimum energy barrier (dashed).

equilibrium geometry relaxes suddenly from bent to linear in the exit channel.

While the model potential is able to reproduce the experimental tunneling rates extremely well, tunneling lifetimes become too short relative to the time-scale of the measurement to determine the fraction of stable radicals near the top of the barrier. Given the 1D approximation used here, the possibility that the actual barrier and tunneling rates deviate from the model at the top of the barrier cannot be ruled out. As the tunneling distance approaches zero the tunneling pathway must approach the minimum energy pathway implying that the extracted barrier shape should approach the shape of the minimum-energy barrier at the saddle-point. The failure to do so could indicate inapplicability of the barrier at these energies, dynamics beyond those explicitly considered in the model, or that the minimum-energy barrier fails to capture the tunneling dynamics at any energy. However, the veracity of the model barrier is supported by the observation in Fig. 3 that the tunneling pathway and the minimum-energy pathway intersect near the saddle point, implying little geometric change as a function of energy for this plane of the PES.

Tunneling lifetimes are computed using the model barrier over its full energy range, shown in Fig. 4 as a function of energy in the dissociation coordinate. It can be seen that in the particularly relevant region near the entrance channel energy of 1.2 eV , the tunneling lifetimes are predicted to be less than 1 psec , similar to the measured lifetime of the HOCO \rightarrow OH + CO process,²⁹ implying that slight collisional stabilization or temporarily bound complexes could lead to non-negligible dissociation through this barrier. Even above the barrier, where dissociation is expected to be facile, frustration due to curvature of the reaction path may also cause tunneling *above* and away from the saddle point energy to become competitive,³⁴ Tunneling rates for the minimum energy barrier, also in Fig. 4, give a lower limit to the tunneling lifetimes and thus can be used in concert with the model lifetimes

to constrain the rates of processes occurring in this energy regime of the PES.

The data presented here can be of direct use in more sophisticated treatments of the tunneling process^{34–36} particularly with regard to the role of vibrational energy distribution in the HOCO* intermediate which is treated crudely in this model. Additionally, the effect of isomerization to *trans*-HOCO acting as a sink for *cis*-HOCO* that would otherwise tunnel is not considered. If this process occurs, the actual tunneling rates could be significantly higher than those predicted by the model barrier. The lowest-energy transition state between *cis*- and *trans*-HOCO is reached by out-of-plane torsional motion of the H atom. Excitation of the torsional mode of HOCO is not expected in photodetachment due to the planarity of both the anion and the neutral and inefficient vibrational redistribution due to the A'' symmetry of the torsional mode, so this transition state should be inactive as a mechanism for the loss of *cis*-HOCO*. However, a poorly characterized higher energy planar isomerization transition state also exists which could result in a reduction in the actual tunneling yield if it is found to have low enough energy. Work on a more detailed transition-state-theory model of the global kinetics on this surface which can accurately reproduce these dissociative photodetachment results should help to further illuminate the role that tunneling plays in the overall dynamics of this reaction.

The authors would like to thank Professors Amit Sinha, John Stanton, and Michael Galperin for helpful discussions and John Stanton for providing the anharmonic vibrational calculations. This work was supported by the United States Department of Energy under Grant No. DE-FG03-98ER14879.

¹R. Berry and P. Lehman, *Annu. Rev. Phys. Chem.* **22**, 47 (1971).

²I. Smith, *Chem. Phys. Lett.* **49**, 112 (1977).

³D. Fulle, H. Hamann, H. Hippler, and J. Troe, *J. Chem. Phys.* **105**, 983 (1996).

⁴J. S. Francisco, J. T. Muckerman, and H.-G. Yu, *Acc. Chem. Res.* **43**, 1519 (2010).

⁵M. Frost, P. Sharkey, and I. Smith, *J. Phys. Chem.* **97**, 12254 (1993).

⁶K. Kudla, G. Schatz, and A. Wagner, *J. Chem. Phys.* **95**, 1635 (1991).

⁷H. Yu and J. Muckerman, *J. Chem. Phys.* **117**, 11139 (2002).

⁸Y. He, E. Goldfield, and S. Gray, *J. Chem. Phys.* **121**, 823 (2004).

⁹M. Aoyagi and S. Kato, *J. Chem. Phys.* **88**, 6409 (1988).

¹⁰H. Yu, J. Muckerman, and T. Sears, *Chem. Phys. Lett.* **349**, 547 (2001).

¹¹M. Lakin, D. Troya, G. Schatz, and L. Harding, *J. Chem. Phys.* **119**, 5848 (2003).

¹²R. Valero, M. van Hemert, and G. Kroes, *Chem. Phys. Lett.* **393**, 236 (2004).

¹³X. Song, J. Li, H. Hou, and B. Wang, *J. Chem. Phys.* **125**, 094301 (2006).

¹⁴M. Alagia, N. Balucani, P. Casavecchia, D. Stranges, and G. Volpi, *J. Chem. Phys.* **98**, 8341 (1993).

¹⁵T. Sears, W. Fawzy, and P. Johnson, *J. Chem. Phys.* **97**, 3996 (1992).

¹⁶J. Petty and C. Moore, *J. Mol. Spectrosc.* **161**, 149 (1993).

¹⁷D. Forney, M. Jacox, and W. Thompson, *J. Chem. Phys.* **119**, 10814 (2003).

¹⁸D. Milligan and M. Jacox, *J. Chem. Phys.* **54**, 927 (1971).

¹⁹T. Oyama, W. Funato, Y. Sumiyoshi, and Y. Y. Endo, in *65th OSU International Symposium on Molecular Spectroscopy*, Columbus, OH, 2010.

²⁰J. Petty and C. Moore, *J. Chem. Phys.* **99**, 47 (1993).

²¹M. Jacox, *J. Chem. Phys.* **88**, 4598 (1988).

²²J. D. Savee, J. E. Mann, and R. E. Continetti, *J. Phys. Chem. A* **114**, 1485 (2010).

²³D. Golden, G. Smith, A. McEwen, C. Yu, B. Eiteneer, M. Frenklach, G. Vaghjani, A. Ravishankara, and F. Tully, *J. Phys. Chem. A* **102**, 8598 (1998).

²⁴D. Medvedev, S. Gray, E. Goldfield, M. Lakin, D. Troya, and G. Schatz, *J. Chem. Phys.* **120**, 1231 (2004).

²⁵S. Zhang, D. M. Medvedev, E. M. Goldfield, and S. K. Gray, *J. Chem. Phys.* **125**, 164312 (2006).

²⁶R. Continetti, *Int. Rev. Phys. Chem.* **17**, 227 (1998).

²⁷T. Clements, R. Continetti, and J. Francisco, *J. Chem. Phys.* **117**, 6478 (2002).

²⁸Z. Lu, Q. Hu, J. E. Oakman, and R. E. Continetti, *J. Chem. Phys.* **126**, 194305 (2007).

²⁹Z. Lu, J. E. Oakman, Q. Hu, and R. E. Continetti, *Mol. Phys.* **106**, 595 (2008).

³⁰C. J. Johnson and R. E. Continetti, *J. Phys. Chem. Lett.* **1**, 1895 (2010).

³¹See supplementary material at <http://dx.doi.org/10.1063/1.3589860> for experimental description, stable fractions, and detailed description of the barrier extraction procedure.

³²W. Miller, *Chem. Rev.* **87**, 19 (1987).

³³M. J. Frisch, G. W. Trucks, H. B. Schlegel *et al.*, GAUSSIAN 09, Revision A.02, Gaussian, Inc., Wallingford, CT, 2009.

³⁴W. Miller, N. Handy, and J. Adams, *J. Chem. Phys.* **72**, 99 (1980).

³⁵R. Skodje, D. Truhlar, and B. Garrett, *J. Phys. Chem.* **85**, 3019 (1981).

³⁶N. Makri and W. H. Miller, *J. Chem. Phys.* **91**, 4026 (1989).

³⁷R. Continetti, D. Cyr, D. Osborn, D. Leahy, and D. Neumark, *J. Chem. Phys.* **99**, 2616 (1993).